Available online at www.sciencedirect.com

ScienceDirect

journal homepage: www.elsevier.com/locate/he

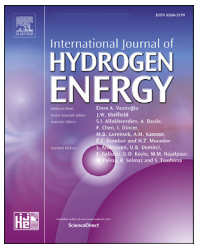

Effects of temperature and pressure fluctuations on exergy loss characteristics of hydrogen auto-ignition processes

Shaoyan Liu [a,b,c], *Jiabo Zhang* [b,*], *Zuoyu Sun* [c], *Dong Han* [a,b,d,**]

[a] China-UK Low Carbon College, Shanghai Jiao Tong University, Shanghai, 200240, China
[b] Key Laboratory for Power Machinery and Engineering, Ministry of Education, Shanghai Jiao Tong University, Shanghai, 200240, China
[c] School of Mechanical, Electronic and Control Engineering, Beijing Jiao Tong University, Beijing, 100044, China
[d] Shanghai Non-carbon Energy Conversion and Utilization Institute, Shanghai, 200240, China

HIGHLIGHTS

- Low-frequency temperature fluctuations decrease exergy loss in H_2 auto-ignition.
- Pressure fluctuations have negligible effects compared to those of temperature.
- Temperature fluctuations promote O_2 consumption and reduce HO_2 and H_2O_2 fractions.
- HO_2 and H_2O_2 consumption reactions and third-body reactions are inhibited.
- Fuel energy conversion may benefit from the addition of temperature fluctuations.

ARTICLE INFO

Article history:
Received 5 March 2023
Received in revised form
5 June 2023
Accepted 7 June 2023
Available online 29 June 2023

Keywords:
Fluctuation
Exergy loss
Hydrogen
Auto-ignition
Chemical kinetics analysis

ABSTRACT

Intake temperature and pressure fluctuations prior to main ignition are one of the reasons affecting the efficiency of internal combustion engines. In this study, the effects of temperature and pressure fluctuations with varied amplitudes and frequencies on the exergy loss of hydrogen auto-ignition processes were numerically investigated in an adiabatic constant-volume system at engine-relevant conditions. The results revealed that the increase in temperature fluctuation amplitudes primarily decreases the exergy loss due to chemical reactions, and the exergy loss due to incomplete combustion remains unchanged. Specifically, the total exergy loss is reduced by approximately 1.5% with a temperature fluctuation amplitude of 100 K at a frequency of 2 ms^{-1}. Furthermore, with the same temperature fluctuation amplitude, increasing the frequency of temperature fluctuation from 2 ms^{-1} to 7 ms^{-1} leads to a 0.7% increase in the total exergy loss. On the other hand, the effects of pressure fluctuation on the exergy loss of hydrogen auto-ignition processes are negligible compared with those of temperature fluctuation. Through chemical kinetic analysis, it is found that temperature fluctuation promotes the consumption pathway of O_2 to generate OH, rather than the collision with H to produce HO_2. Consequently, the reduced mole fraction of HO_2 inhibits the related HO_2-consumption reactions, including $HO_2+H=OH + OH$ and $HO_2+HO_2=H_2O_2+O_2$. Moreover, with temperature fluctuation, due to the lower fraction of third-body collision molecules, H_2O, the reactivity of the third-body reaction, $H + O_2+M=HO_2+M$, is decreased. The reduced reaction rates of

* *Corresponding author.*
** *Corresponding author.* Key Laboratory for Power Machinery and Engineering, Ministry of Education, Shanghai Jiao Tong University, Shanghai, 200240, China.
E-mail addresses: zhangjiabo@sjtu.edu.cn (J. Zhang), dong_han@sjtu.edu.cn (D. Han).
https://doi.org/10.1016/j.ijhydene.2023.06.084

these reactions lead to decreased total exergy loss, indicating that the fuel energy conversion process may benefit from temperature fluctuation.

Introduction

As the main power machinery in the field of transportation, the research on high-efficiency internal combustion (IC) engines has attracted extensive attention [1–3]. One effective approach to improving the efficiency of IC engines is by optimizing their intake parameters, such as preheating and intake boost [4–6]. For instance, Bendu et al. [7] analyzed the effects of intake temperature on the combustion efficiency of an ethanol-fueled homogeneous charge compression ignition (HCCI) engine. The results indicated that increasing the intake temperature led to an improvement in combustion efficiency, primarily due to the accelerated oxidation reaction of the fuel caused by the higher in-cylinder temperature. Similarly, Jiang et al. [8] investigated the effects of intake pressure on gasoline compression ignition (GCI) combustion. It was discovered that increasing the intake pressure resulted in improved indicated thermal efficiency (ITE) due to the advanced combustion phase and shortened combustion duration, which benefited from the more complete combustion and faster flame propagation speed, especially under low-load conditions.

However, the intake process of engines is transient with various types of scalar fluctuations, including temperature [9–12], pressure [13–17], mixture composition [18–21], and scalar dissipation rate [22]. Temperature and pressure are the primary factors of interest among the various thermodynamic variables since reactions are highly sensitive to these parameters, necessitating further investigation. To identify the temperature fluctuation amplitude, Bürkle et al. [23] measured the in-cylinder gas temperature using tunable diode laser absorption spectroscopy (TDLAS). The maximum temperature fluctuation amplitude was found to be 60 K prior to the top dead center (TDC). For an acetone/n-heptane-fueled HCCI engine, pressure fluctuations were also observed by Aydoğan [24]. The magnitude of pressure fluctuations was found to be higher at lower equivalence ratio conditions, with a maximum amplitude of 1.0 atm near the TDC. Some studies [9–17] have indicated that these temperature and pressure fluctuations may have some impacts on the ignition characteristics. For instance, Bansal et al. [9] explored the impact of unsteady temperature fluctuation on ignition delay times for a homogeneous hydrogen-air mixture through a zero-dimensional simulation, across a range of frequencies. The ignition delay was found to exhibit a harmonic response to the temperature fluctuation in both the high- and low-temperature ignition regimes. As an extension of this fundamental study, Song et al. [10] employed the computational singular perturbation (CSP) tools to investigate the effects of imposed temperature fluctuation on the response of an igniting mixture in a homogeneous hydrogen-air system. It was discovered that the ignition delay time consistently decreased when the system was subjected to temperature fluctuations, regardless of the amplitude and frequency of the imposed fluctuation. These studies demonstrated that temperature fluctuation had a significant impact on ignition characteristics, leading to alterations in ignition delay times. Further, using multi-dimensional simulations, Im et al. [11] and Pal et al. [12] observed that the presence of temperature fluctuations caused the ignition mode to transit from spontaneous auto-ignition to deflagration.

Changes in the above ignition characteristics potentially affect the corresponding combustion efficiency [25–31]. A few studies have attempted to examine how temperature and pressure fluctuations affect combustion efficiency based on the first law of thermodynamics. For instance, Dong et al. [32] investigated the effects of intake temperature fluctuation on the combustion efficiency of an ethanol/diesel dual-fuel engine. The results showed that temperature fluctuation enhanced the cycle-to-cycle variation, thus improving the combustion efficiency under low load conditions. Eng [33] studied the effects of combustion-generated pressure fluctuation on the performance of a single-cylinder engine operating in HCCI combustion mode. It was discovered that the pressure fluctuation caused by the rapid combustion rates in the HCCI combustion mode resulted in increased engine noise, thereby leading to lower combustion efficiency.

Note that the above analyses were based solely on the first law of thermodynamics, which focused on the thermal efficiency of fuel energy converted to output work, leaving the evaluation of the fuel availability unaddressed [34]. In IC engines, the irreversible combustion process results in an approximate one-third loss of the initial fuel availability, which restricts the engine efficiency improvement [35]. Therefore, analysis based on the second law of thermodynamics which examines the maximum useful work of IC engines should be highlighted for their efficiency optimization [36–38]. As above-mentioned, intake temperature and pressure have a significant impact on the energy conversion processes. To assess their impacts broadly, numerous efforts were made to evaluate the magnitude of combustion-induced exergy loss under different temperature and pressure conditions. For instance, Feng et al. [39] analyzed the effects of intake conditions on the exergy loss of a low-temperature combustion (LTC) engine with a toluene reference fuel. They discovered that a higher intake temperature led to a higher temperature rising rate and a lower exergy loss. Conversely, an increase in intake pressure did not significantly affect exergy loss. To give further insights into the change of exergy loss, chemical kinetic analyses are generally coupled to identify the primary sources of irreversibility during combustion processes, such as chemical reaction, heat conduction, mass diffusion, and viscous dissipation [40–44]. By this means, Zhang et al. [45] investigated the effects of temperature and fraction stratification on the exergy loss of dimethyl ethyl and ethanol auto-ignition processes. The results showed

that the stratification of temperature and fuel composition caused by the intake fluctuation could result in a deflagration combustion mode, which smoothed the combustion process and reduced the total exergy loss, primarily due to the decrease of exergy loss by chemical reactions. Similarly, Li et al. [46] compared the exergy loss for engines operating in HCCI, reactivity-controlled compression ignition (RCCI), and conventional diesel combustion (CDC) modes. It was found that the exergy loss in CDC mode was the highest due to the enhanced heat conduction and mass transfer, caused by the excessive gradients of in-cylinder temperature and fuel fraction. In the above analysis, only the effects of temperature and pressure and their non-uniform distribution before TDC on the exergy loss were considered, lacking consideration of the intake temperature and pressure fluctuations. While these studies provided the effect of temperature and pressure fluctuations on combustion efficiency based solely on the first law of thermodynamics, the effect of temperature and pressure fluctuations on exergy loss remains unclear. More fundamental investigations are needed to understand how temperature and pressure fluctuations affect exergy loss based on the second law of thermodynamics, as another important efficiency evaluation matric.

Therefore, the objectives of this study are two-fold: (1) to investigate the effects of temperature and pressure fluctuations with different amplitudes and frequencies on the exergy loss of hydrogen auto-ignition processes, and (2) to provide reasons for the change in the exergy loss through chemical kinetic analysis. Given the push towards carbon neutrality, hydrogen is regarded as a leading candidate for an ultimate energy source. As the simplest carbon-free fuel, it boasts high energy density and calorific value while producing the cleanest combustion product compared to other fuels [47–49]. Therefore, hydrogen was selected as an example in this study. Employing the second law of thermodynamics, the effects of different levels of temperature and pressure fluctuations on the exergy loss characteristics of hydrogen auto-ignition processes were investigated using a zero-dimensional adiabatic constant-volume model. The sum of the exergy loss due to chemical reactions and incomplete combustion was considered the total exergy loss. The results showed that temperature fluctuation reduced the total exergy loss, which was primarily due to the decreased exergy loss by chemical reactions. On the contrary, pressure fluctuation had a negligible effect on the exergy loss. Furthermore, chemical kinetic analysis, including reaction pathway analysis, rate of production analysis, and reaction rate analysis, was used to provide the underlying reasons for the above phenomena.

Methodology

The hydrogen mechanism used in this paper includes 9 species and 20 individual reactions [50], which is well-validated to predict the ignition-related characteristics as demonstrated in Refs. [51,52]. A zero-dimensional homogeneous closed constant-volume adiabatic combustion model is constructed using Cantera [53]. The computational configuration is the same as those used in our previous works [41,54]. The initial temperature and pressure of the model are set to 1000 K and 40 atm, respectively, to simulate the high temperature and pressure of the engine combustion chamber at TDC. The equivalence ratio of the mixture is set to 1.0. As shown in Fig. 1 (a), the temperature and pressure fluctuation functions are constructed using a sine function:

$$y = y_0 + A\sin(2\pi f t) \quad (1)$$

where y represents temperature or pressure, A and f are the amplitude and frequency of fluctuation, respectively. The subscript 0 refers to the initial value (1000 K for temperature and 40 atm for pressure).

From a thermodynamic perspective, the state of a system is determined by temperature, pressure, and concentration (T, P, and X_i). Enthalpy and entropy are properties that are dependent on these variables. In this study, ΔT and ΔP are introduced in Eq. (1), which, in combination with chemical

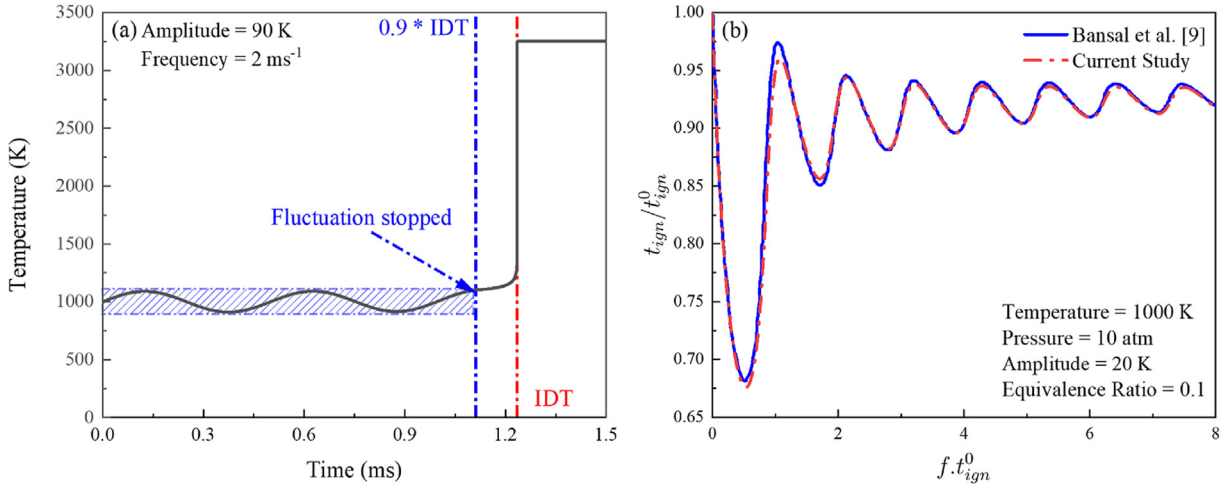

Fig. 1 – (a) Auto-ignition process of hydrogen/air mixtures with temperature fluctuation; (b) Ignition delay time compared with the results of Bansal et al. [9] under a constant temperature amplitude of 20 K for hydrogen/air mixtures at an initial pressure of 10 atm, initial temperature of 1000 K and equivalence ratio of 0.1.

reaction kinetics, affect the combustion process and lead to changes in the thermodynamic state (T', P', and X_i'). In this study, the reference state is defined at a temperature of 25 °C (298 K) and a pressure of 1.0 atm. The standard enthalpy and entropy of different species can be obtained from the NASA database and serve as a reference for the following calculations [55]. Based on the reference state, the enthalpy and entropy at different temperatures and pressures for a specific mixture are calculated by Eqs. (2) and (3).

$$H' = U' + P'V' \tag{2}$$

where H' is enthalpy, U' is internal energy, P' is pressure, and V' is volume.

$$dS' = \frac{C_v'}{T'} dT' \tag{3}$$

where C_v' represents the heat capacity at constant volume, which is a state variable depending on T, P, and X_i.

The effects of amplitude and frequency of temperature and pressure fluctuation on the exergy loss are investigated by varying A (ranging from 0 K to 100 K for temperature and 0 atm to 1.0 atm for pressure) and f (ranging from 1 ms^{-1} to 7 ms^{-1}). Note that, the selection of the temperature and pressure fluctuation amplitudes and frequencies is based on data from engine experiments [23,24]. During the engine operation, the intake disturbance mainly exists during the intake valve opening period. Therefore, to mimic the intake processes of engines, fluctuations are introduced only within the first 90% of the ignition delay period. Note that, this also helps to avoid the forced change in temperature and pressure in the combustion process caused by the introduced disturbance, and the ignition delay time (IDT) is defined as the time when the heat release rate reaches its peak, as shown in Fig. 1 (a) (taking the temperature fluctuation as an example). To validate the accuracy of our model, a comparison is made between the computed ignition delay time in this study with that obtained from Bansal et al. [9] in the presence of temperature fluctuations with varied frequencies (see Fig. 1 (b)). The initial temperature is 1000 K, the initial pressure is 10 atm, the equivalence ratio is 0.1, and the amplitude of temperature fluctuations is 20 K. Good agreement between the literature data and the results provides the accuracy of the model.

It has been indicated that the inherent thermodynamic irreversibility involved in the conventional combustion process significantly limits the conversion of fuel energy into work [35].

From the view of the first law of thermodynamics, the energy conservation equation is as

$$c_v \frac{dT}{dt} + v \sum_{i=1}^{i} u_i \omega_i W_i = 0 \tag{4}$$

where c_v is the constant-volume specific heat capacity, u_i is the specific internal energy of the ith species, v is the specific volume, ω_i is the mole production rate of the ith species and W_i is the molecular weight of the ith species.

The entropy conservation equation from the second law of thermodynamics is as follows:

$$\Delta S = (\Delta S)_Q + (\Delta S)_W + (\Delta S)_M + S_{gen} \tag{5}$$

where ΔS, $(\Delta S)_Q$, $(\Delta S)_W$, $(\Delta S)_M$ and S_{gen} stand for the entropy change, thermal entropy flow, work entropy flow, mass entropy flow, and entropy generation, respectively.

As the system in this study is zero-dimensional homogeneous closed constant-volume adiabatic, $(\Delta S)_Q$, $(\Delta S)_W$, and $(\Delta S)_M$ in Eq. (5) can all be ignored, simplifying the formula to only consider chemical entropy generation. Consequently, Eq. (5) could be simplified to Eq. (6) as:

$$\Delta S = S_{gen} \tag{6}$$

According to the Gouy-Stodla equation [56], the irreversibility in the combustion process is calculated as

$$I = T_0 S_{gen} = T_0 \Delta S \tag{7}$$

where I is the irreversibility of combustion and ΔS stands for entropy change.

The entropy generation equation [57,58] can be simplified as

$$\rho \frac{ds}{dt} = -\sum_i \frac{\mu_i \omega_{i,j}}{T} \tag{8}$$

where ρ is the mole density, μ_i is the chemical potential of the ith species, and $\omega_{i,j}$ is the mole production rate of the ith species due to the jth reaction.

The irreversibility rate of the j^{th} reaction can be obtained by Eq. (9).

$$Ex_{loss}rate_j = -\frac{T_0}{T} \sum_i \mu_i \omega_{i,j} \tag{9}$$

where T is the temperature of the reaction.

The chemical potential in Eq. (9) can be calculated as

$$\mu_i = h_i - Ts_i + RT \ln\left(\frac{x_i p}{p_0}\right) \tag{10}$$

where h_i and x_i are the specific enthalpy and mole fraction of the ith species, respectively.

The exergy loss caused by the jth reaction within the time step of Δt can be expressed by Eq. (11). Specifically, the advanced time step used in this study is small enough; therefore, the changes in thermodynamic quantities (T, P, X_i) within this time step are negligible. This assumption allows us to compute the corresponding quantities, such as μ_i and $\omega_{i,j}$, as shown in Eq. (9) [59].

$$AEx_{loss} = Ex_{loss}rate_j \Delta t \tag{11}$$

The percentage of exergy loss due to chemical reactions can be calculated as

$$Ex_{loss} = \frac{\sum_n AEx_{loss}}{Ech_{fuel,0}} \times 100\% \tag{12}$$

where $Ech_{fuel,0}$ is the initial chemical exergy of the fuel, and n is the total number of calculations.

The chemical exergy of the fuel ($C_aH_bO_c$) is defined as the initial exergy as Eq. (13).

$$Ech_{fuel,0} = \left(G_F + \left(a + \frac{b}{4} - \frac{c}{2}\right) G_{O_2} - aG_{CO_2} - \frac{b}{2} G_{H_2O}\right)(T_0, P_0) \tag{13}$$

where $G(T_0, P_0)$ is the Gibbs free energy of different species at T_0 and P_0, respectively.

The percentage of exergy loss due to incomplete combustion is

$$\text{Eincomp}_{\text{loss}} = \frac{Ech_{end}}{Ech_{fuel,0}} \times 100\% \quad (14)$$

where Ech_{end} is the exergy of the mixture at the end of the reaction.

The total exergy loss is the sum of the exergy loss due to chemical reactions and incomplete combustion. The percentage of total exergy loss is calculated as

$$\text{Total loss} = \text{Ex}_{\text{loss}} + \text{Eincomp}_{\text{loss}} \quad (15)$$

Results and discussions

Figs. 2 (a and b) and (c and d) describe the exergy loss of hydrogen auto-ignition processes due to chemical reactions and incomplete combustion as well as the total exergy loss with different levels of temperature and pressure fluctuations, respectively. Note that the fluctuation frequencies of temperature and pressure fluctuations both range from 1 ms^{-1} to 7 ms^{-1}, and the fluctuation amplitudes range from 0 K to 100 K for temperature and 0 atm to 1.0 atm for pressure. As shown in Fig. 2 (a), when the temperature fluctuation amplitude increases from 0 K to 100 K with a constant fluctuation frequency of 2 ms^{-1}, the exergy loss due to chemical reactions monotonically decreases from 9.4% to 7.9%, while the exergy

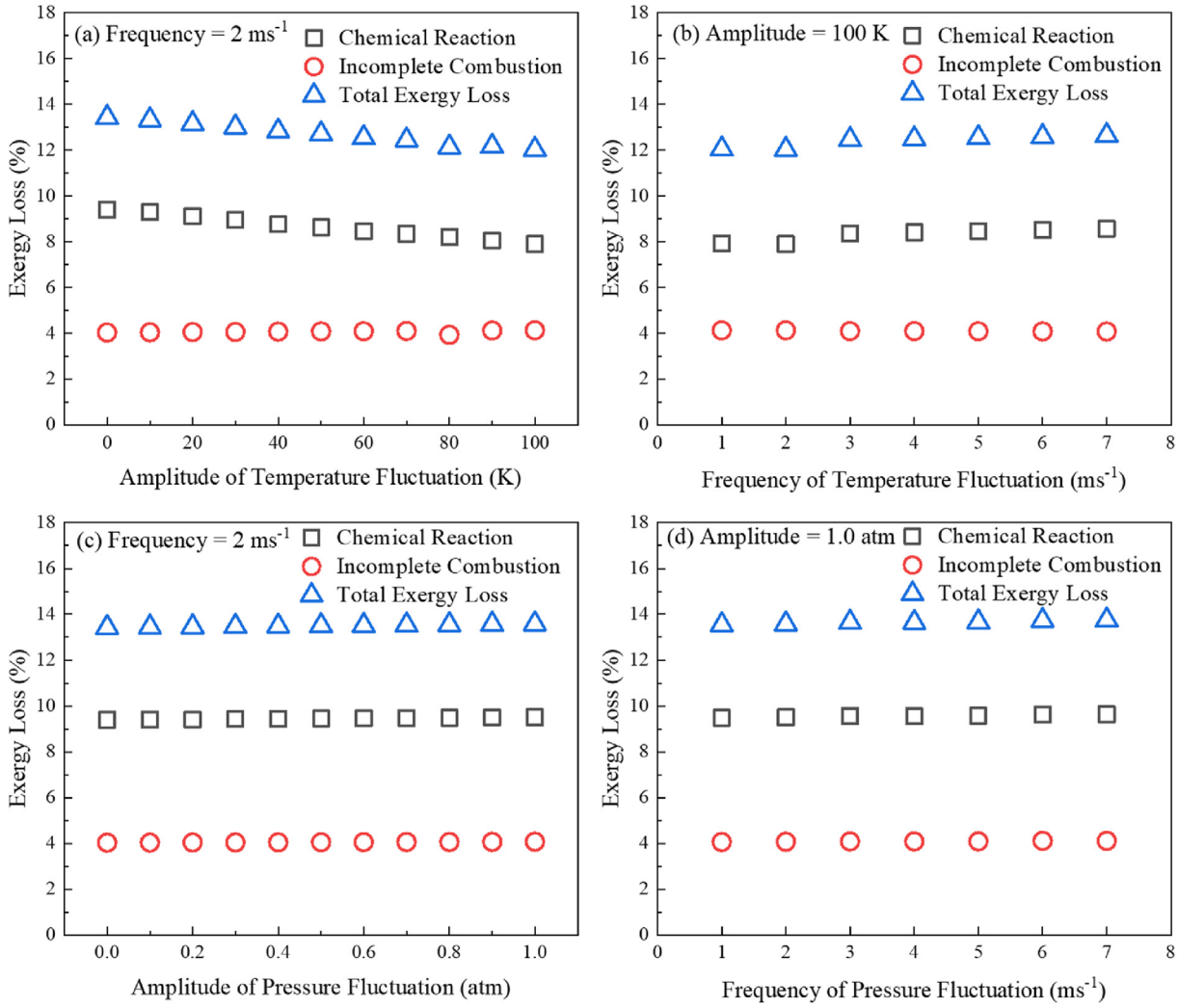

Fig. 2 – The change of exergy loss caused by: (a) temperature fluctuation amplitude ranging from 0 K to 100 K with a constant frequency of 2 ms^{-1}, (b) temperature fluctuation frequency ranging from 1 ms^{-1} to 7 ms^{-1} with a constant amplitude of 100 K, (c) pressure fluctuation amplitude ranging from 0 atm to 1.0 atm with a constant frequency of 2 ms^{-1} and (d) pressure fluctuation frequency varied from 1 ms^{-1} to 7 ms^{-1} with a constant amplitude of 1.0 atm for hydrogen/air mixtures at an initial pressure of 40 atm, initial temperature of 1000 K and equivalence ratio of 1.0.

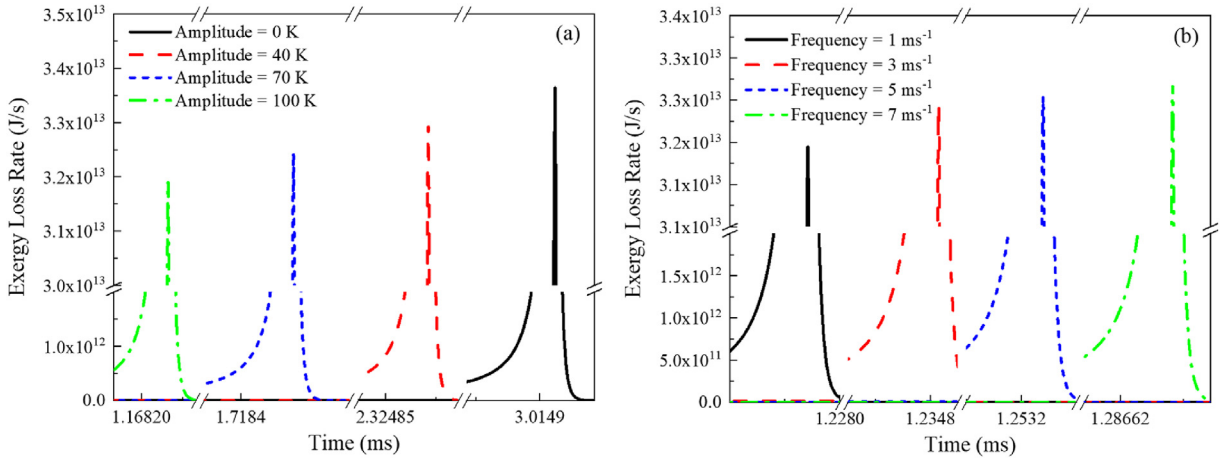

Fig. 3 – Exergy loss rate histories of hydrogen auto-ignition processes with (a) different temperature fluctuation amplitude and (b) different temperature fluctuation frequency at an initial pressure of 40 atm, an initial temperature of 1000 K and an equivalence ratio of 1.0.

loss due to incomplete combustion remains nearly unchanged. As shown in Fig. 2 (b), the exergy loss due to chemical reactions increases from 7.9% to 8.6% as the temperature fluctuation frequency increases from 1 ms^{-1} to 7 ms^{-1} with a constant temperature fluctuation amplitude of 100 K, while the change of exergy loss due to incomplete combustion is negligible. On the contrary, as shown in Figs. 2 (c) and (d), pressure fluctuation has less obvious effects on the exergy loss compared to those of temperature fluctuation. With varied amplitude and frequency of pressure fluctuation, the exergy loss induced by chemical reactions and incomplete combustion only experiences a slight change of 0.2%. Due to the negligible influence of pressure fluctuation on the exergy loss, the effects of temperature fluctuation on exergy loss characteristics of hydrogen auto-ignition processes are focused in the following.

According to Eq. (11), the exergy loss due to chemical reactions is simultaneously determined by the exergy loss rate and chemical reaction duration. To analyze the results from Fig. 2, the exergy loss rate histories of hydrogen auto-ignition processes with different temperature fluctuation amplitudes (ranging from 0 K to 100 K in Fig. 3 (a)) and temperature fluctuation frequencies (ranging from 1 ms^{-1} to 7 ms^{-1} in Fig. 3 (b)) are illustrated in Fig. 3. It is readily observed that the ignition delay time is promoted with the increase in temperature fluctuation amplitude, and it is retarded with the increase in temperature fluctuation frequency. Compared with temperature fluctuation amplitude, the temperature fluctuation frequency has less impact on the ignition delay time. Furthermore, temperature fluctuation amplitude and frequency have little effect on the duration of the chemical reaction. As a result, the change in exergy loss due to chemical reactions observed in Fig. 2 is primarily caused by the peak value of exergy loss rates. Specifically, the peak value of the exergy loss rate is observed to decrease with an increased temperature fluctuation amplitude and increase with an increased temperature fluctuation frequency, which corresponds to the observation in Fig. 2. Therefore, a detailed analysis of the impact of temperature fluctuations with varying amplitudes and frequencies on exergy loss is necessary.

The varied exergy loss rates due to chemical reactions depicted in Fig. 3 are believed to be the consequent results of the changed reaction pathway. To provide a more detailed analysis of the chemical pathways responsible for the exergy loss of homogeneous mixtures in the presence of temperature fluctuations, Fig. 4 as such compares the reaction pathway of hydrogen/air mixture combustion under different conditions. The percentage near the arrow represents the proportion of reactant passing through the pathway. Three representative Cases 1–3 (Case 1: amplitude = 0 K, frequency = 0 ms^{-1}; Case 2: amplitude = 100 K, frequency = 2 ms^{-1}; Case 3: amplitude = 100 K, frequency = 7 ms^{-1}) are selected.

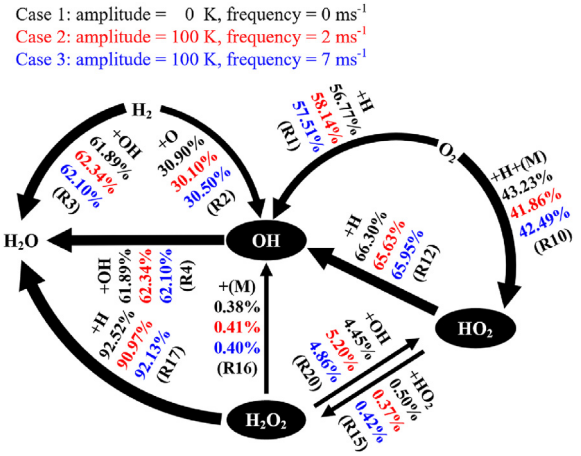

Fig. 4 – Reaction pathway for the hydrogen auto-ignition processes in Cases 1–3 (Case 1: amplitude = 0 K, frequency = 0 ms^{-1}; Case 2: amplitude = 100 K, frequency = 2 ms^{-1}; Case 3: amplitude = 100 K, frequency = 7 ms^{-1}) at an initial pressure of 40 atm, an initial temperature of 1000 K and an equivalence ratio of 1.0 (Black number: Case 1; Red number: Case 2; Blue number: Case 3). (For interpretation of the references to color in this figure legend, the reader is referred to the Web version of this article.)

Table 1 – The contributions of all individual reactions to the total exergy loss of hydrogen auto-ignition processes for Cases 1–3 (the contribution less than 0.1% is represented by " - ").

Reactions		Case 1	Case 2	Case 3
Amplitude (A) and frequency (f) of temperature fluctuation		$A = 0$ K $f = 0$ ms^{-1}	$A = 100$ K $f = 2$ ms^{-1}	$A = 100$ K $f = 7$ ms^{-1}
Reaction No.	Exergy loss due to individual reaction			
R1	$H + O_2$=O + OH	0.95%	0.89%	0.92%
R2	$O + H_2$=H + OH	0.40%	0.38%	0.39%
R3	H_2+OH=H_2O + H	1.87%	1.54%	1.68%
R4	OH + OH=O + H_2O	–	–	–
R5	H_2+M=H + H + M	–	–	–
R6	O + O + M=O_2+M	–	–	–
R7	O + H + M=OH + M	0.22%	0.23%	0.22%
R8	H_2O + M = H + OH + M	0.27%	0.27%	0.27%
R9	H_2O + H_2O=H + OH + H_2O	0.56%	0.53%	0.54%
R10	H + O_2+M=HO_2+M	1.70%	1.33%	1.49%
R11	HO_2+H=H_2+O_2	0.28%	0.26%	0.27%
R12	HO_2+H=OH + OH	1.57%	1.41%	1.49%
R13	HO_2+O=O_2+OH	0.15%	0.14%	0.15%
R14	HO_2+OH=H_2O + O_2	0.18%	0.16%	0.17%
R15	HO_2+HO_2=H_2O_2+O_2	0.30%	0.18%	0.23%
R16	H_2O_2+M = OH + OH + M	0.53%	0.26%	0.37%
R17	H_2O_2+H=H_2O + OH	0.15%	0.11%	0.13%
R18	H_2O_2+H=HO_2+H_2	–	–	–
R19	H_2O_2+O=OH + HO_2	–	–	–
R20	H_2O_2+OH=HO_2+H_2O	–	–	–
Exergy loss due to all reactions		9.40%	7.90%	8.56%

According to the reaction pathway as shown in Fig. 4, it is found that temperature fluctuation primarily influences the hydrogen-consumption and oxygen-consumption reaction pathway. Specifically, temperature fluctuation leads more H_2 to react with OH radicals producing H_2O (R3 seen in Table 1). It also enhances the proportion of H + O_2=O + OH (R1) for the consumption of oxygen, producing more OH radicals instead of HO_2 from R10. Note that the increased OH radicals produced by the chain branching reaction R1 may enhance the reactivity of the reaction system. The hydroperoxyl radical, HO_2, formed by R10 is then consumed by the two HO_2-consuming reactions, namely HO_2+H=OH + OH (R12) and HO_2+HO_2=H_2O_2+O_2 (R15), to produce OH and H_2O_2. It is observed that both R12 and R15 are suppressed due to the temperature fluctuation. Moreover, with temperature fluctuation, more H_2O_2 is consumed to produce OH (R16), further increasing the mole fraction of OH radicals. Additionally, as the fluctuation frequency increases (from Case 2 to Case 3), the effects of temperature fluctuation become less significant.

The contributions of all individual reactions in Cases 1–3 to the total exergy loss are further listed in Table 1. It is readily observed that the temperature fluctuation primarily influences the exergy loss due to R3, R10, R12, R15, and R16 as highlighted. Note that the branching ratios of these reactions also experience significant changes in the reaction pathway as shown in Fig. 4. Specifically, R3 is the main hydrogen-consumption reaction, R10 is the primary oxygen-consumption reaction, R12 and R15 are HO_2-consumption reactions, and R16 is an H_2O_2-consumption reaction. Temperature fluctuation affects the reaction pathway of the above reactions and further affects their contributions to the total exergy loss. The exergy loss of these reactions decreases as the temperature fluctuation amplitude increases from 0 K to 100 K. On the contrary, as the temperature fluctuation frequency increased from 2 ms^{-1} to 7 ms^{-1}, the exergy loss of these reactions increases. As the main contributors to the total exergy loss, the exergy loss of these reactions is further analyzed as follows.

A detailed analysis of the chemical reaction kinetics for the aforementioned reactions was conducted. According to the reaction pathway as shown in Fig. 4, H_2 is consumed primarily by OH, followed by O (R2). As the main contributor to the consumption of hydrogen, the reaction rates of R3 in Cases 1–3 are compared in Fig. 5. It is found that the reaction rate of

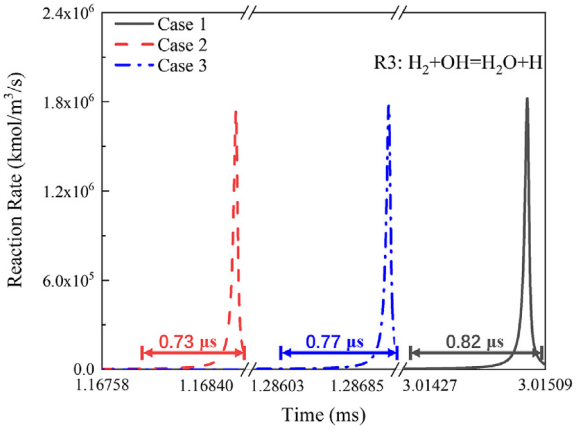

Fig. 5 – Reaction rate histories of R3 in Cases 1–3 (Case 1: amplitude = 0 K, frequency = 0 ms^{-1}; Case 2: amplitude = 100 K, frequency = 2 ms^{-1}; Case 3: amplitude = 100 K, frequency = 7 ms^{-1}) of hydrogen auto-ignition processes at an initial pressure of 40 atm, an initial temperature of 1000 K and an equivalence ratio of 1.0.

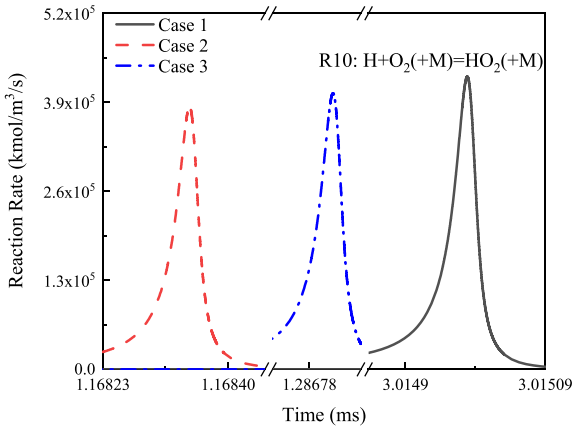

Fig. 6 – Reaction rate histories of R10 in Cases 1–3 (Case 1: amplitude = 0 K, frequency = 0 ms^{-1}; Case 2: amplitude = 100 K, frequency = 2 ms^{-1}; Case 3: amplitude = 100 K, frequency = 7 ms^{-1}) of hydrogen auto-ignition processes at an initial pressure of 40 atm, an initial temperature of 1000 K and an equivalence ratio of 1.0.

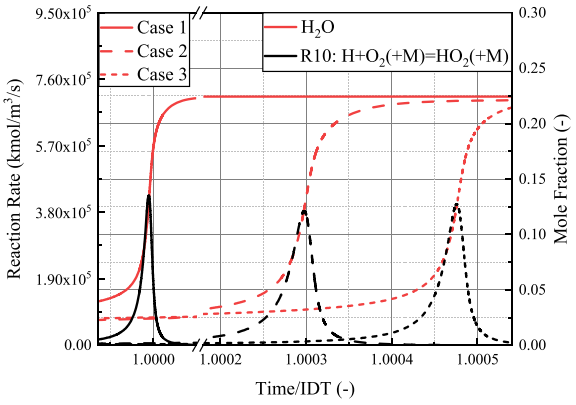

Fig. 7 – The mole fraction of H_2O (red) and reaction rate (black) histories of hydrogen auto-ignition processes in Cases 1–3 (Case 1: amplitude = 0 K, frequency = 0 ms^{-1}; Case 2: amplitude = 100 K, frequency = 2 ms^{-1}; Case 3: amplitude = 100 K, frequency = 7 ms^{-1}) at an initial pressure of 40 atm, an initial temperature of 1000 K and an equivalence ratio of 1.0. (For interpretation of the references to color in this figure legend, the reader is referred to the Web version of this article.)

R3 experiences a slight change with temperature fluctuation. However, as shown in Fig. 5, the reaction duration of R3 in Cases 1–3 (the time interval between the reaction rate reaching its 1% maximum value) is found to be decreased. According to Eq. (11), the shorter duration of R3 caused by temperature fluctuation is the primary reason for the exergy loss decrease. Moreover, the time interval of R3 increases for Case 3 on the basis of Case 2, and the effects of temperature fluctuation as such become less significant as the frequency of fluctuations increases.

The H atom produced in R3 further reacts with O_2 to form HO_2 (R10). Fig. 6 shows the reaction rate histories of $H + O_2 + M = HO_2 + M$ (R10) in Cases 1–3. It is revealed that the reaction rate of R10 decreases with temperature fluctuation. This is consistent with the observation in Fig. 4 that the branching ratio of R10 is decreased with temperature fluctuation. As a third-body reaction, three third-body substances, namely H_2, H_2O, and O_2, could collide with the reactants to produce HO_2, with collision efficiencies of 2.0, 14.0, and 0.78, respectively. Note that the mole fraction of H_2O has the greatest influence on the reaction rate of R10 since it has the highest collision efficiency. Fig. 7 as such plots the evolutions of the H_2O mole fraction for Cases 1–3. At the instant of the maximum reaction rates in these three cases, the mole fractions of H_2O are 0.120, 0.113, and 0.116, respectively. As a result, the reduction in the fraction of H_2O causes a decrease in the reaction rate of R10, leading to a decrease in its exergy loss according to Eq. (11), and this influence is reduced by increasing the frequency of temperature fluctuation.

According to the reaction pathway depicted in Fig. 4, HO_2 produced by R10 continues to generate H_2O_2 and O_2 (R15) or reacts with H to produce OH (R12). The reaction rate histories of $HO_2 + H = OH + OH$ (R12) and $HO_2 + HO_2 = H_2O_2 + O_2$ (R15) in Cases 1–3 are shown in Fig. 8, and the corresponding mole fractions of HO_2 are illustrated in Fig. 9. It is observed from Fig. 8 that the reaction rates of R12 and R15 decrease with temperature fluctuation. Furthermore, as shown in Fig. 9, temperature fluctuation also causes a decrease in the mole fraction of HO_2. This is consistent with the observation in reaction pathway analysis (as shown in Fig. 4) that R10 is suppressed due to temperature fluctuation, resulting in less O_2 consumed to generate HO_2. The exergy loss of R12 and R15 is reduced as a result of the decrease in reaction rates caused by the HO_2 fraction reduction. Consequently, the contributions of R12 and R15 to the exergy loss by chemical reactions are reduced, and this effect decreases as the frequency of temperature fluctuation increases.

H_2O_2 produced by R15 is then consumed to generate OH (R16). The reaction rate histories of $H_2O_2 + M = OH + OH + M$ (R16) and the corresponding mole fractions of H_2O_2 in Cases 1–3 are shown in Figs. 10 and 11, respectively. It is observed from Fig. 10 that the reaction rate of R16 decreases with temperature fluctuation. Furthermore, as illustrated in Fig. 11, temperature fluctuation causes a decrease in the mole fraction of H_2O_2. As the only H_2O_2 generation reaction, the decrease in the reaction rate of R15 leads to a decrease in the mole fraction of H_2O_2, which may decline the reaction rate of R16. On the other hand, as a third-body reaction, five third-body substances, namely H_2, H_2O, N_2, H_2O_2, and O_2, could collide with the reactants to produce OH, with collision efficiencies of 3.7, 7.5, 1.5, 7.7, and 1.2, respectively. Note that the mole fractions of H_2O and H_2O_2 have the greatest impact on the reaction rate of R16 due to the higher collision efficiency. The reduction in the fractions of H_2O (as shown in Fig. 7) and H_2O_2 (as shown in Fig. 11) is as such reasoning for the decrease in the reaction rate of R16. As a result, due to the decrease in reaction rate caused by either the H_2O_2 fraction reduction or the lower fractions of third-body collision molecules, the contribution of R16 to the exergy loss by chemical reactions is reduced, and this effect decreases as the frequency of temperature fluctuation increases.

Through the above analysis, it is summarized that temperature fluctuation primarily affects the hydrogen-consumption and oxygen-consumption reaction pathway,

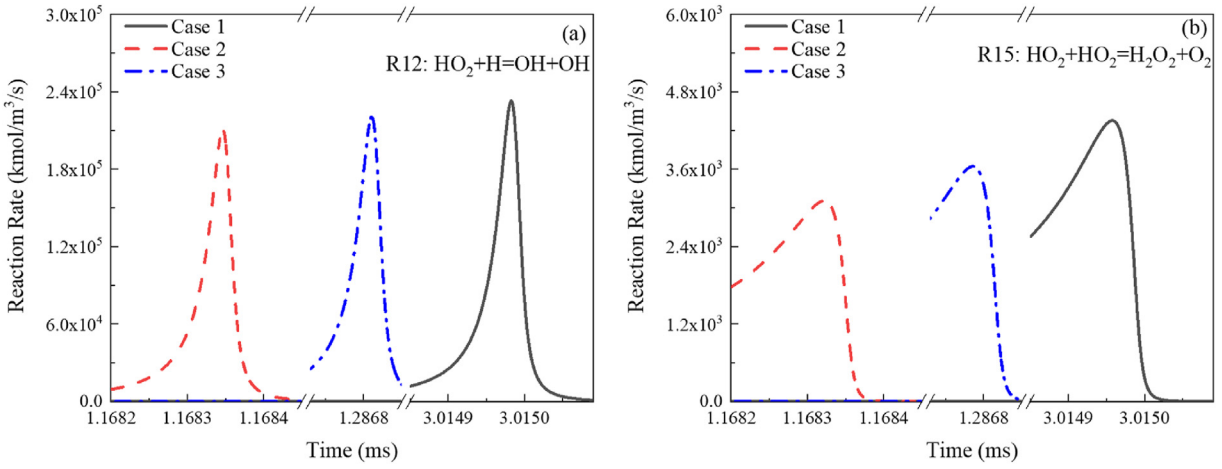

Fig. 8 – Reaction rate histories of R12 and R15 in Cases 1–3 (Case 1: amplitude = 0 K, frequency = 0 ms^{-1}; Case 2: amplitude = 100 K, frequency = 2 ms^{-1}; Case 3: amplitude = 100 K, frequency = 7 ms^{-1}) of hydrogen auto-ignition processes at an initial pressure of 40 atm, an initial temperature of 1000 K and an equivalence ratio of 1.0.

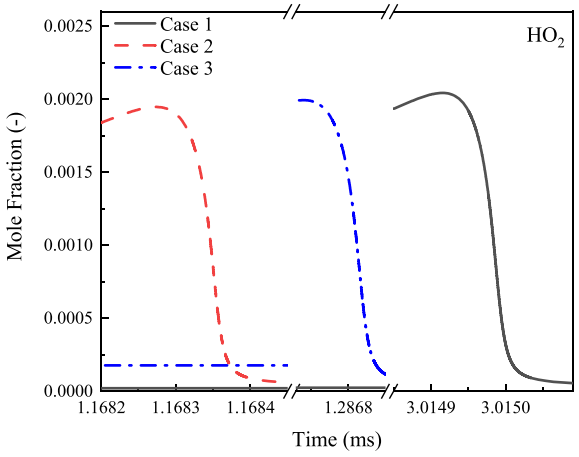

Fig. 9 – HO_2 mole fraction histories in Cases 1–3 (Case 1: amplitude = 0 K, frequency = 0 ms^{-1}; Case 2: amplitude = 100 K, frequency = 2 ms^{-1}; Case 3: amplitude = 100 K, frequency = 7 ms^{-1}) of hydrogen auto-ignition processes at an initial pressure of 40 atm, an initial temperature of 1000 K and an equivalence ratio of 1.0.

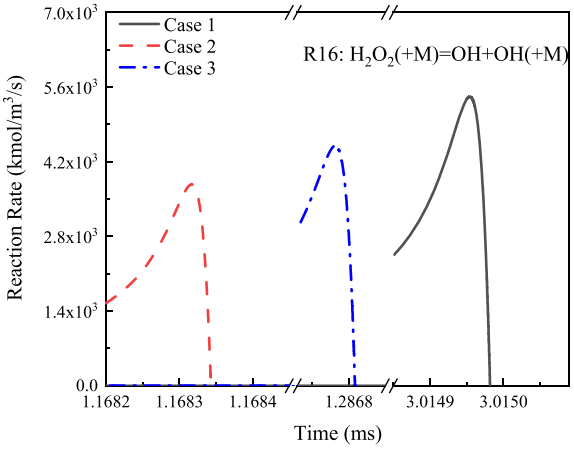

Fig. 10 – Reaction rate histories of R16 in Cases 1–3 (Case 1: amplitude = 0 K, frequency = 0 ms^{-1}; Case 2: amplitude = 100 K, frequency = 2 ms^{-1}; Case 3: amplitude = 100 K, frequency = 7 ms^{-1}) of hydrogen auto-ignition processes at an initial pressure of 40 atm, an initial temperature of 1000 K and an equivalence ratio of 1.0.

promoting the generation of active radicals such as OH, O, and H, and as such enhances the reactivity of the reaction system. This, in turn, influences the reaction rates, resulting in a reduction in exergy loss. Furthermore, it was also found that the increase in frequency weakened the effects introduced by the temperature fluctuation.

Note that, in practical engines, exergy loss is caused by multiple factors, including heat conduction, mass diffusion, viscous dissipation, chemical reaction, and incomplete combustion. Among these factors, the chemical reaction is found to play the dominant role [46]. However, all the above factors could affect the energy conversion process. Therefore, in this study, as the main contributor to exergy loss, the chemical reaction is isolated and focused using the 0-D model. This strategy allows us to emphasize the effects of temperature and pressure fluctuations on combustion-induced irreversibility, without considering other complex phenomena such as mass transport and heat dissipation. As indicated by the previous studies, temperature and pressure fluctuations may influence the exergy loss from several other aspects in practical engines. For example, the addition of fluctuations has an impact on the cycle-to-cycle variation, resulting in a decline in combustion efficiency [32]. This decrease can potentially lead to increased exergy losses associated with incomplete combustion components. Moreover, temperature and pressure fluctuations could influence the combustion phase, leading to changes in the heat transfer process and potential variations in exergy loss attributable to heat conduction [33]. However, the limitations of simplified 0-D simulations prevent a comprehensive understanding of these phenomena, which needs further investigation.

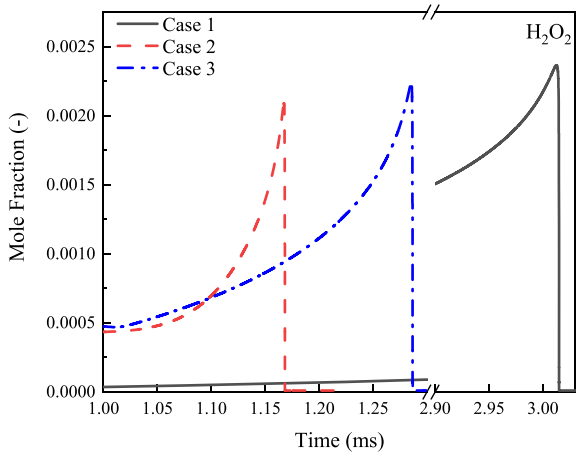

Fig. 11 – H_2O_2 mole fraction histories in Cases 1–3 (Case 1: amplitude = 0 K, frequency = 0 ms^{-1}; Case 2: amplitude = 100 K, frequency = 2 ms^{-1}; Case 3: amplitude = 100 K, frequency = 7 ms^{-1}) of hydrogen auto-ignition processes at an initial pressure of 40 atm, an initial temperature of 1000 K and an equivalence ratio of 1.0.

Conclusions

In this study, the effects of amplitude and frequency of temperature and pressure fluctuations on the energy conversion of hydrogen auto-ignition processes are numerically studied in an adiabatic constant-volume system using the second law of thermodynamics. A parametric study is performed by varying the fluctuation amplitude (ranging from 0 K to 100 K for temperature and 0 atm to 1.0 atm for pressure) and fluctuation amplitude frequency (ranging from 1 ms^{-1} to 7 ms^{-1}). Further, employing chemical kinetic analysis, the underlying mechanisms for how temperature fluctuation decreases the exergy loss were revealed. The main conclusions are as follows.

1. The temperature fluctuation reduces the exergy loss, primarily due to the decrease of the exergy loss induced by chemical reactions, and the reduction effect becomes more significant with higher temperature fluctuation amplitude and lower temperature fluctuation frequency. On the contrary, the effects of pressure fluctuation on the exergy loss are negligible.
2. With temperature fluctuation, more O_2 tends to react with H to produce OH (R1), thus leading to an increase in the mole fraction of OH. Due to the increased mole fraction of OH, the chain propagation reaction, $H_2+OH=H_2O+H$ (R3), is promoted. On the other hand, as another O_2-consumption reaction competing with R1, $H+O_2+M=HO_2+M$ (R10) is suppressed. Therefore, the mole fraction of HO_2 is reduced with temperature fluctuation, and further decreases the mole fraction of H_2O_2 from R15 ($HO_2+HO_2=H_2O_2+O_2$).
3. The above reactions with changes in reaction pathway experience significant changes in the exergy loss. With temperature fluctuation, the reduction of HO_2 and H_2O_2 inhibits the HO_2-consumption reactions, such as $HO_2+H=OH+OH$ (R12) and $HO_2+HO_2=H_2O_2+O_2$ (R15), as well as the H_2O_2-consumption reaction, $H_2O_2+M=OH+OH+M$ (R16). Moreover, due to the lower fractions of third-body collision molecules, the reactivity of the third-body reaction, $H+O_2+M=HO_2+M$ (R10), is inhibited. Reduced reaction rates of these reactions result in a lower total exergy loss, indicating that the fuel energy conversion process may benefit from temperature fluctuation with lower fluctuation frequency and higher fluctuation amplitude.

Declaration of competing interest

The authors declare that they have no known competing financial interests or personal relationships that could have appeared to influence the work reported in this paper.

Acknowledgments

This research work is supported by the National Key R&D Program of China (No. 2022YFE0209000), the National Natural Science Foundation of China (Grant Nos. 52106261 and 52022058), and the Postdoctoral Research Foundation of China (Grant Nos. 2022M712042 and 2022T150403).

REFERENCES

[1] Zhao T, Ren Z, Yang K, Sun T, Shi L, Huang Z, et al. Combustion and emissions of RP-3 jet fuel and diesel fuel in a single-cylinder diesel engine. Front Energy 2021. https://doi.org/10.1007/s11708-021-0787-3.
[2] Li X, Li D, Pei Y, Peng Z. Optimising microscopic spray characteristics and particle emissions in a dual-injection spark ignition (SI) engine by changing GDI injection pressure. Int J Engine Res 2023;24:1290–9.
[3] Zhang J, Huang Z, Han D. Effects of mechanism reduction on the exergy losses analysis in n-heptane autoignition processes. Int J Engine Res 2020;21:1764–77.
[4] Mohamed Ibrahim M, Ramesh A. Investigations on the effects of intake temperature and charge dilution in a hydrogen fueled HCCI engine. Int J Hydrogen Energy 2014;39:14097–108.
[5] Wu H, Zhang Y, Mi S, Zhao W, He Z, Qian Y, et al. A methodology for regulating fuel stratification and improving fuel economy of GCI mode via double main-injection strategy. Front Energy 2023:1–14. https://doi.org/10.1007/s11708-022-0859-z.
[6] Xia C, Zhao T, Fang J, Zhu L, Huang Z. Experimental study of stratified lean burn characteristics on a dual injection gasoline engine. Front Energy 2022;16:900–15.
[7] Bendu H, Sivalingam M. Experimental investigation on the effect of charge temperature on ethanol fueled HCCI combustion engine. J Mech Sci Technol 2016;30:4791–9.
[8] Jiang C, Li Z, Liu G, Qian Y, Lu X. Achieving high efficient gasoline compression ignition (GCI) combustion through the cooperative-control of fuel octane number and air intake conditions. Fuel 2019;242:23–34.
[9] Bansal G, Im HG, Lee S-R. Auto-ignition of a homogeneous hydrogen–air mixture subjected to unsteady temperature fluctuations. Combust Theor Model 2009;13:413–25.

[10] Song W, Tingas E-A, Lee S-R, Im HG. A computational analysis of autoignition of H_2/air mixture with temperature fluctuations using computational singular perturbation. In: 26th international colloquium on the dynamics of explosions and reactive systems; 2017 [Boston, MA, USA].
[11] Im HG, Pal P, Wooldridge MS, Mansfield AB. A regime diagram for autoignition of homogeneous reactant mixtures with turbulent velocity and temperature fluctuations. Combust Sci Technol 2015;187:1263–75.
[12] Pal P, Valorani M, Arias PG, Im HG, Wooldridge MS, Ciottoli PP, et al. Computational characterization of ignition regimes in a syngas/air mixture with temperature fluctuations. Proc Combust Inst 2017;36:3705–16.
[13] Terashima H, Matsugi A, Koshi M. End-gas autoignition behaviors under pressure wave disturbance. Combust Flame 2019;203:204–16.
[14] Liberman MA, Ivanov MF, Valiev DM, Eriksson LE. Hot spot formation by the propagating flame and the influence of EGR on knock occurrence in SI engines. Combust Sci Technol 2006;178:1613–47.
[15] Pan J, Shu G, Zhao P, Wei H, Chen Z. Interactions of flame propagation, auto-ignition and pressure wave during knocking combustion. Combust Flame 2016;164:319–28.
[16] Terashima H, Matsugi A, Koshi M. Origin and reactivity of hot-spots in end-gas autoignition with effects of negative temperature coefficients: relevance to pressure wave developments. Combust Flame 2017;184:324–34.
[17] Pan J, Wei H, Shu G, Chen R. Effect of pressure wave disturbance on auto-ignition mode transition and knocking intensity under enclosed conditions. Combust Flame 2017;185:63–74.
[18] Sankaran R, Im HG. Characteristics of auto-ignition in a stratified iso-octane mixture with exhaust gases under homogeneous charge compression ignition conditions. Combust Theor Model 2005;9:417–32.
[19] Sankaran R, Im HG. Dynamic flammability limits of methane/air premixed flames with mixture composition fluctuations. Proc Combust Inst 2002;29:77–84.
[20] Bansal G, Im HG. Time scales in unsteady premixed flame extinction with composition fluctuations. Combust Flame 2007;150:404–8.
[21] Tomidokoro T, Yokomori T, Im HG, Ueda T. Characteristics of counterflow premixed flames with low frequency composition fluctuations. Combust Flame 2020;212:13–24.
[22] Bansal G, Im HG, Lee S-R. Effects of scalar dissipation rate fluctuations on autoignition of hydrogen/air mixture. AIAA J 2009;47:468–72.
[23] Bürkle S, Biondo L, Ding C-P, Honza R, Ebert V, Böhm B, et al. In-cylinder temperature measurements in a motored IC engine using TDLAS. Flow, Turbul Combust 2018;101:139–59.
[24] Aydoğan B. Combustion characteristics, performance and emissions of an acetone/n-heptane fuelled homogenous charge compression ignition (HCCI) engine. Fuel 2020;275:117840.
[25] Adams CA, Loeper P, Krieger R, Andrie MJ, Foster DE. Effects of biodiesel–gasoline blends on gasoline direct-injection compression ignition (GCI) combustion. Fuel 2013;111:784–90.
[26] Labeckas G, Slavinskas S, Kanapkienė I. The individual effects of cetane number, oxygen content or fuel properties on the ignition delay, combustion characteristics, and cyclic variation of a turbocharged CRDI diesel engine – Part 1. Energy Convers Manag 2017;148:1003–27.
[27] Shahridzuan Abdullah I, Khalid A, Jaat N, Saputra Nursal R, Koten H, Karagoz Y. A study of ignition delay, combustion process and emissions in a high ambient temperature of diesel combustion. Fuel 2021;297:120706.
[28] Tat ME. Cetane number effect on the energetic and exergetic efficiency of a diesel engine fuelled with biodiesel. Fuel Process Technol 2011;92:1311–21.
[29] Jena J, Misra RD. Effect of fuel oxygen on the energetic and exergetic efficiency of a compression ignition engine fuelled separately with palm and karanja biodiesels. Energy 2014;68:411–9.
[30] Yan F, Su W. A promising high efficiency RM-HCCI combustion proposed by detail kinetics analysis of exergy losses. SAE Tech Pap 2015. 2015-01-1751, https://doi.org/10.4271/2015-01-1751.
[31] Ma B, Yao A, Yao C, Wu T, Wang B, Gao J, et al. Exergy loss analysis on diesel methanol dual fuel engine under different operating parameters. Appl Energy 2020;261:114483.
[32] Dong S, Cheng X, Ou B, Liu T, Wang Z. Experimental and numerical investigations on the cyclic variability of an ethanol/diesel dual-fuel engine. Fuel 2016;186:665–73.
[33] Eng J. Characterization of pressure waves in HCCI combustion. 2002. SAE Technical Paper 2002-01-2859.
[34] Alkidas AC. The application of availability and energy balances to a diesel engine. J Eng Gas Turbines Power 1988;110:462–9.
[35] Dunbar WR, Lior N. Sources of combustion irreversibility. Combust Sci Technol 1994;103:41–61.
[36] Caton JA. The thermodynamic characteristics of high efficiency, internal-combustion engines. Energy Convers Manag 2012;58:84–93.
[37] Zheng J, Caton JA. Second law analysis of a low temperature combustion diesel engine: effect of injection timing and exhaust gas recirculation. Energy 2012;38:78–84.
[38] Rakopoulos CD, Giakoumis EG. Second-law analyses applied to internal combustion engines operation. Prog Energy Combust Sci 2006;32:2–47.
[39] Feng H, Wang X, Zhang J. Study on the effects of intake conditions on the exergy destruction of low temperature combustion engine for a toluene reference fuel. Energy Convers Manag 2019;188:241–9.
[40] Nishida K, Takagi T, Kinoshita S. Analysis of entropy generation and exergy loss during combustion. Proc Combust Inst 2002;29(1):869–74.
[41] Zhang J, Huang Z, Han D. Exergy losses in auto-ignition processes of DME and alcohol blends. Fuel 2018;229:116–25.
[42] Liu Y, Zhang J, Ju D, Huang Z, Han D. Analysis of exergy losses in laminar premixed flames of methane/hydrogen blends. Int J Hydrogen Energy 2019;44:24043–53.
[43] Liu Y, Chen J, Qiu Z, Chen Z, Han D. Second-law thermodynamic analysis on premixed syngas flames. Int J Exergy 2020;32:174–85.
[44] Liu Y, Zhang J, Ju D, Shi L, Han D. Second-law thermodynamic analysis on non-premixed counterflow methane flames with hydrogen addition. J Therm Anal Calorimetry 2020;139:2577–83.
[45] Zhang J, Luong MB, Pérez FEH, Han D, Im HG, Huang Z. Exergy loss characteristics of DME/air and ethanol/air mixtures with temperature and concentration fluctuations under HCCI/SCCI conditions: a DNS study. Combust Flame 2021;226:334–46.
[46] Li Y, Jia M, Kokjohn SL, Chang Y, Reitz RD. Comprehensive analysis of exergy destruction sources in different engine combustion regimes. Energy 2018;149:697–708.
[47] Balli O, Caliskan H. Energy, exergy, environmental and sustainability assessments of jet and hydrogen fueled military turbojet engine. Int J Hydrogen Energy 2022;47:26728–45.
[48] Bakar RA, Widudo Kadirgama K, Ramasamy D, Yusaf T, Kamarulzaman MK, et al. Experimental analysis on the performance, combustion/emission characteristics of a DI diesel engine using hydrogen in dual fuel mode. Int J

Hydrogen Energy 2022. https://doi.org/10.1016/j.ijhydene.2022.04.129.
[49] Varuvel EG, Thiyagarajan S, Sonthalia A, Prakash T, Awad S, Aloui F, et al. Some studies on reducing carbon dioxide emission from a CRDI engine with hydrogen and a carbon capture system. Int J Hydrogen Energy 2022;47:26746–57.
[50] Burke MP, Chaos M, Ju Y, Dryer FL, Klippenstein SJ. Comprehensive H_2/O_2 kinetic model for high-pressure combustion. Int J Chem Kinet 2012;44:444–74.
[51] Krüger O, Terhaar S, Paschereit CO, Duwig C. Large eddy simulations of hydrogen oxidation at ultra-wet conditions in a model gas turbine combustor applying detailed chemistry. J Eng Gas Turbines Power 2013;135(2):021501.
[52] Hashemi H, Christensen JM, Gersen S, Glarborg P. Hydrogen oxidation at high pressure and intermediate temperatures: experiments and kinetic modeling. Proc Combust Inst 2015;35:553–60.
[53] Liu D, Wang H, Liu H, Zheng Z, Zhang Y, Yao M. Identification of factors affecting exergy destruction and engine efficiency of various classes of fuel. Energy 2020;211:118897.
[54] Zhang J, Huang Z, Min K, Han D. Dilution, thermal, and chemical effects of carbon dioxide on the exergy destruction in n-heptane and iso-octane autoignition processes: a numerical study. Energy & Fuels 2018;32:5559–70.
[55] Zehe M, Gordon S, McBride B, Cap. A computer code for generating tabular thermodynamic functions from NASA Lewis coefficients. Cleveland, OH: National Aeronautics and Space Administration, Glenn Research Center; 2002.
[56] Bejan A, Kestin J. Entropy Generation through heat and fluid flow. J Appl Mech 1983;50:475.
[57] Chen S, Li J, Han H, Liu Z, Zheng C. Effects of hydrogen addition on entropy generation in ultra-lean counter-flow methane-air premixed combustion. Int J Hydrogen Energy 2010;35:3891–902.
[58] Briones AM, Mukhopadhyay A, Aggarwal SK. Analysis of entropy generation in hydrogen-enriched methane–air propagating triple flames. Int J Hydrogen Energy 2009;34:1074–83.
[59] Lebon G, Jou D, Casas-Vázquez J. Understanding non-equilibrium thermodynamics. Springer; 2008.